Proc. 13th GAMM-Seminar Kiel on Numerical
Treatment of Multi-Scale Problems, 1/97.

Boundary Integral Solution of Laplace's Equation with Highly Varying Coefficients *

Johannes Tausch and Jacob White
Research Laboratory of Electronics
Massachusetts Institute of Technology
Cambridge, MA 02139
USA

Abstract

A boundary integral formulation for Laplace's equation with piecewise constant coefficients is discussed. When the dynamic range of the coefficients is large, the solution of the integral equation can have different scales, which results in large discretization errors on components where the solution is small. We introduce a perturbation technique to avoid different scaling. The analysis of this approach shows that the Galerkin discretization error of the method can be bounded independently of the coefficients. Numerical experiments support the analysis.

1 Introduction

Potential problems involving composite materials arise frequently in applications ranging from electrostatics and magnetostatics to thermal conductivity. The governing equation common to many of these problems is Laplace's equation with piecewise constant coefficients reflecting different material properties. It is known from finite element calculations that large jumps of the coefficient function lead to inaccurate results and ill-conditioned linear systems. This is one of the concerns that lead to the development of the mixed finite element method and to the first-order least squares method [4], [7].

Surprinsingly, there is not much work available on boundary integral formulations for this kind of problem and the existing literature does not address the numerical difficulties that arise if the dynamical range of the coefficients is large, see e.g., [1] and the literature cited therein.

In this paper we investigate the cause of large numerical errors for a model problem that arises when calculating capacitances of conductor systems in multiple dielectric materials. We will demonstrate that the poor approximation properties of a straight-forward application of the boundary element method is due to different scales of the solution on the Dirichlet surface and the interfaces of different media.

*This work is supported by the NSF under contract ECS-9301-189

To avoid having to solve for unknowns which may vary by many orders of magnitude, we will introduce a perturbation technique of the original boundary integral formulation. The first problem corresponds to letting the large coefficient approach infinity and involves only large-scale unknowns on the interface. To account for the finite coefficient a perturbation equation on both surfaces is solved which only involves small-scale unknowns. We conclude with some preliminary numerical experiments comparing the original integral formulation with the perturbation method.

2 Boundary Integral Formulation

We consider here the model problem

$$\begin{aligned} \nabla \cdot (a \nabla u) &= 0 && \text{in } \mathbf{R}^3 \setminus S_c \\ u &= f_c && \text{on } S_c \\ u &= \mathcal{O}(\tfrac{1}{|x|}) && \text{as } |x| \to \infty , \end{aligned} \tag{1}$$

where S_c denotes the boundary of a bounded domain $C \subset \mathbf{R}^3$. The scalar coefficient function a is positive and for simplicity we require that $a(x)$ assumes only two distinct values, namely

$$a(x) = \begin{cases} a_0 & x \in D_0 , \\ a_1 & x \in D_1 . \end{cases}$$

Furthermore, we assume that the domain D_1 contains the larger coefficient, is simply connected and bounded, and that $\bar{C} \subset D_1$. In applications the component D_0 corresponds to free space, where the coefficient is fixed. The interface of D_1 and D_0 is denoted by $S_d = \partial D_0$. A typical geometry is depicted in Figure 1.

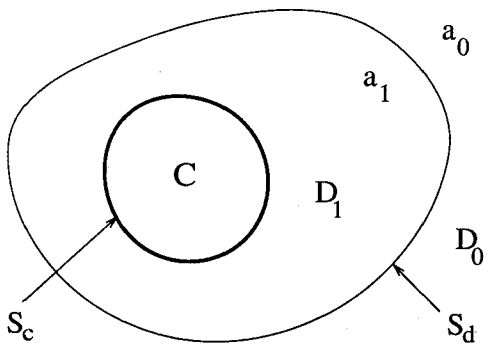

Figure 1: Problem Geometry

To avail ourselves of the standard theory of elliptic boundary value problems, we assume that $S = S_c \cup S_d$ is a smooth surface. Under these assumptions it is known that for the function $f_c \in H^{1/2}(S_c)$ there exists a unique solution $u \in H^1_{\text{loc}}(\mathbf{R}^3)$.

To cast the partial differential equation (1) as a boundary integral equation we note that the potential u is harmonic in each connected component of $\mathbf{R}^3 \setminus S$. This suggests that u may be written as the super-position of surface potentials

$$u(x) = V\sigma(x) := V_c\sigma_c(x) + V_d\sigma_d(x) , \qquad x \in \mathbf{R}^3 , \tag{2}$$

where V_c and V_d are the single-layer operators on the boundary surface S_c and the interface S_d, respectively, defined by

$$V_c\sigma_c(x) = \int_{S_c} G(x,y)\,\sigma_c(y)\,dS_y\,, \qquad x \in \mathbf{R}^3\,,$$

and

$$V_d\sigma_d(x) = \int_{S_d} G(x,y)\,\sigma_d(y)\,dS_y\,, \qquad x \in \mathbf{R}^3\,.$$

The kernel $G(x,y)$ is the Green's function for the Laplace operator in three dimensions

$$G(x,y) = \frac{1}{4\pi}\frac{1}{|x-y|}\,.$$

The unknown densities σ_c and σ_d are determined by the boundary conditions. On S_c we can stipulate that

$$V\sigma(x) = f_c(x)\,, \quad x \in S_c\,.$$

On the interface the potential defined by (2) must satisfy the following continuity condition of the flux $a\nabla u$

$$a_1\frac{\partial u^-}{\partial n} = a_0\frac{\partial u^+}{\partial n} \qquad \text{on } S_d\,. \tag{3}$$

Here n denotes the normal of the interface which is oriented into D_0, and $u^\pm = u(x \pm 0n)$. The normal derivative of the single layer potential satisfies the jump relation

$$\frac{\partial u^\pm}{\partial n}(x) = \left(\mp\frac{1}{2} + K'\right)\sigma(x)\,, \qquad x \in S\,, \tag{4}$$

were K' is the adjoint of the double-layer operator and is given by

$$K'\sigma(x) = \int_S \frac{\partial}{\partial n_x}G(x,y)\,\sigma(y)\,dS_y\,, \qquad x \in S\,.$$

The operators K_c', K_d' are defined similarly for potentials due densities on S_c and S_d. Combining (2), (3), and (4), the following system of integral equations for σ_c and σ_d can be derived

$$\begin{aligned} V_c\sigma_c(x) + V_d\sigma_d(x) &= f_c(x)\,, \quad x \in S_c \\ K_c'\sigma_c(x) + \left(\tfrac{1}{2\lambda} + K_d'\right)\sigma_d(x) &= 0\,, \quad x \in S_d\,. \end{aligned} \tag{5}$$

The parameter λ is given by

$$\lambda = \frac{a_1 - a_0}{a_1 + a_0}\,. \tag{6}$$

The orientation of the normals ensures that $0 < \lambda < 1$.

Subtracting the jump relations (4) for both sides of the surface yields the important relation between the density and the jump in the normal derivative of the potential

$$\sigma = \frac{\partial u^-}{\partial n} - \frac{\partial u^+}{\partial n}\,. \tag{7}$$

Formulation (5) has appeared previously in the engineering literature [6], where it is usually referred to as the equivalent charge formulation.

3 Highly Varying Coefficients

In this section we will analyze the solution behavior of the equivalent charge formulation. With our assumptions on the surface the mapping properties of the boundary integral operators of potential theory are well-known. In particular, for $\alpha \in \mathbf{R}$,

$$\begin{aligned} V_c &: H^{-1/2+\alpha}(S_c) \rightarrow H^{1/2+\alpha}(S_c) \quad \text{is elliptic,} \\ K_c' &: H^{-1/2+\alpha}(S_c) \rightarrow H^{-1/2+\alpha}(S_d) \quad \text{is compact,} \\ V_d &: H^{-1/2+\alpha}(S_d) \rightarrow H^{1/2+\alpha}(S_c) \quad \text{is compact,} \\ K_d' &: H^{-1/2+\alpha}(S_d) \rightarrow H^{-1/2+\alpha}(S_d) \quad \text{is compact.} \end{aligned}$$

As usual, the Sobolev spaces $H^p(S)$ are defined for $p \geq 0$ by

$$\begin{aligned} H^p(S) := \Big\{ f : \|f\|^2_{H^p(S)} := \sum_{|\alpha| \leq [p]} \int_S |D^\alpha f|^2 \\ + \sum_{|\alpha|=[p]} \int_S \int_S \frac{|D^\alpha f(x) - D^\alpha f(y)|^2}{|x-y|^{2(p-[p])+2}} dS_x dS_y < \infty \Big\}, \end{aligned} \tag{8}$$

and for $p < 0$ by duality with respect to the L_2-scalar product.

For the subsequent analysis it will be useful to rewrite the equivalent charge formulation (5) as the sum of the elliptic operator $\mathcal{S}_\lambda : H^{-1/2+\alpha}(S) \rightarrow H^{1/2+\alpha}(S_c) \times H^{-1/2+\alpha}(S_d)$ and the compact operator $\mathcal{K} : H^{-1/2+\alpha}(S) \rightarrow H^{1/2+\alpha}(S_c) \times H^{-1/2+\alpha}(S_d)$

$$(\mathcal{S}_\lambda + \mathcal{K})\sigma = f, \tag{9}$$

where

$$\mathcal{S}_\lambda = \begin{bmatrix} V_c & 0 \\ 0 & \frac{1}{2\lambda} \end{bmatrix}, \quad \mathcal{K} = \begin{bmatrix} 0 & V_d \\ K_c' & K_d' \end{bmatrix}, \quad \sigma = \begin{bmatrix} \sigma_c \\ \sigma_d \end{bmatrix} \text{ and } f = \begin{bmatrix} f_c \\ f_d \end{bmatrix}.$$

In equation (5) we have $f_d = 0$, but sometimes it will be important to consider a more general $f_d \in H^{-1/2+\alpha}(S_d)$. The main purpose of this article is to discuss coefficients of large ratios. For that, set $a_0 = 1$ and assume $a_1 \gg 1$, which is equivalent to $\lambda \geq \lambda_0$ for a positive λ_0. In the limit $\lambda \rightarrow 1$ integral equation (5) assumes the form

$$(\mathcal{S}_1 + \mathcal{K})\rho = f. \tag{10}$$

In view of Green's Theorem we see that the potential generated by a solution of (10)

$$v(x) := V_c\rho_c(x) + V_d\rho_d(x), \quad x \in \mathbf{R}^3$$

solves the boundary value problem

$$\begin{aligned} \Delta v &= 0 && \text{in } \mathbf{R}^3 \setminus S \\ v &= f_c && \text{on } S_c \\ v^+ &= v^- && \text{on } S_d \\ \tfrac{\partial v}{\partial n}^- &= 0 && \text{on } S_d \\ v &= \mathcal{O}(\tfrac{1}{|x|}) && \text{as } |x| \rightarrow \infty. \end{aligned} \tag{11}$$

Boundary value problems (1) and (11) are well-posed problems. Since the density is the jump of the normal derivative across the boundary, integral equations (5) and (10) are also well posed. This is made more precise in the next Theorem. Note that throughout this article $\gamma, \gamma_1, \gamma_2, \ldots$ denote constants independent of λ, whose actual values may change from line to line.

Theorem 1 *For $\lambda_0 < \lambda \leq 1$ and $f \in H^{1/2+\alpha}(S_c) \times H^{-1/2+\alpha}(S_d)$ the solution of (9) exists uniquely in $H^{-1/2+\alpha}(S)$ and depends continuously on the data. That is, there are constants $\gamma_1, \gamma_2 > 0$, independent of λ such that*

$$\gamma_1 \|f\|_{H^{1/2+\alpha}(S_c)\times H^{-1/2+\alpha}(S_d)} \leq \|\sigma\|_{H^{-1/2}(S)} \leq \gamma_2 \|f\|_{H^{1/2+\alpha}(S_c)\times H^{-1/2+\alpha}(S_d)} \,. \tag{12}$$

Proof. Injectivity follows immediately from the unique existence of the solution of (1) and (11). Namely, if σ is a solution for $f = 0$, then the resulting potential $u = V_c\sigma_c + V_d\sigma_d$ solves (1) and must therefore vanish. Because of the jump relation (4) the density σ vanishes as well and injectivity of the operator $\mathcal{S}_\lambda + \mathcal{K}$ follows.

For the existence and continuous dependence of the data, note that the operator $\mathcal{S}_\lambda \colon H^{-1/2+\alpha}(S) \to H^{1/2+\alpha}(S_c) \times H^{-1/2+\alpha}(S_d)$ has a continuous inverse. Thus (9) may be rewritten in the form

$$(I + \mathcal{S}_\lambda^{-1}\mathcal{K})\sigma = \mathcal{S}_\lambda^{-1} f \,, \tag{13}$$

Since the operator $\mathcal{S}_\lambda^{-1}\mathcal{K} \colon H^{-1/2+\alpha}(S) \to H^{-1/2+\alpha}(S)$ is compact the existence of the solution $\sigma \in H^{-1/2+\alpha}(S)$ follows from Riesz-Fredholm theory.

It remains to show that γ_1,γ_2 in (12) are independent of λ. For that, note that $\mathcal{S}_\lambda \to \mathcal{S}_1$ uniformly and $\|\mathcal{S}_\lambda\| \leq \gamma_1$, furthermore $\mathcal{S}_\lambda^{-1} \to \mathcal{S}_1^{-1}$ uniformly with $\|\mathcal{S}_\lambda^{-1}\| \leq \gamma_2$ and hence $\|I + \mathcal{S}_\lambda^{-1}\mathcal{K}\| \leq \gamma_3$. Since taking the inverse is continuous it follows $(I + \mathcal{S}_\lambda^{-1}\mathcal{K})^{-1} \to (I + \mathcal{S}_1^{-1}\mathcal{K})^{-1}$ in $H^{-1/2}(S)$ and $\|(I + \mathcal{S}_\lambda^{-1}\mathcal{K})^{-1}\| \leq \gamma_4$. Thus we may estimate

$$\|\sigma\|_{H^{-1/2+\alpha}(S)} = \|(I + \mathcal{S}_\lambda^{-1}\mathcal{K})^{-1}\mathcal{S}_\lambda^{-1} f\|_{H^{-1/2+\alpha}(S)} \leq \gamma_4\gamma_2 \|f\|_{H^{1/2+\alpha}(S_c)\times H^{-1/2+\alpha}(S_d)} \,,$$

and

$$\|f\|_{H^{1/2+\alpha}(S_c)\times H^{-1/2+\alpha}(S_d)} = \|\mathcal{S}_\lambda(I + \mathcal{S}_\lambda^{-1}\mathcal{K})\sigma\|_{H^{1/2+\alpha}(S_c)\times H^{-1/2+\alpha}(S_d)} \leq \gamma_1\gamma_3 \|\sigma\|_{H^{-1/2+\alpha}(S)} \,.$$

This asserts (12). □

Subtracting equations (9) and (10) gives

$$(\mathcal{S}_\lambda + \mathcal{K})(\rho - \sigma) = \frac{\lambda - 1}{2\lambda}\rho_d \,.$$

Thus we see from the last theorem that the solutions for the same right hand side converge to each other as $\lambda \to 1$, i.e., for $\lambda_0 < \lambda \leq 1$

$$\|\rho - \sigma\|_{H^{-1/2+\alpha}(S)} \leq \frac{\gamma}{a_1} \|\rho\|_{H^{-1/2+\alpha}(S)} . \tag{14}$$

In many physical situations one is interested in the quantities $a\sigma$ (free charge) and $a\nabla u$ (flux). Estimates for $a\sigma$ will depend on the constant part and its orthogonal complement

$$\bar{f}_c = \frac{1}{|S_c|} \int_{S_c} f_c \,, \tag{15}$$

$$f_c^\perp = f_c - \bar{f}_c \,. \tag{16}$$

of the right hand side f_c. In the following we will denote the solutions of equations (9) and (10) for right hand sides $f = [\bar{f}_c, 0]$ and $f = [f_c^\perp, 0]$ by $\bar{\sigma}$, $\bar{\rho}$, $\rho^\perp$ and $\sigma^\perp$, respectively.

Lemma 1 *There are constants $\gamma_1, \gamma_2 > 0$ such that*

$$\gamma_1 \|f_c^\perp\|_{H^{1/2+\alpha}(S_c)} \leq \|\rho_c\|_{H^{-1/2+\alpha}(S_c)} \leq \gamma_2 \|f_c^\perp\|_{H^{1/2+\alpha}(S_c)} \tag{17}$$

hold for the solution of (10) with right hand side $f = [f_c, 0]$.

Proof. If the right hand side of boundary value problem (11) is constant, then the solution v is constant in $\mathbf{R}^3 \setminus D_0$ and the density ρ_c vanishes because of the jump relations (4). For a non-constant right hand side the solution of (11) has a nonzero gradient. From Green's theorem

$$\int_{D_1} |\nabla v|^2 = \int_{S_c} \rho_c f_c$$

it then follows that $\rho_c \neq 0$. Thus the the map $T : f_c \mapsto \rho_c$ is an isomorphism of the spaces $H^{1/2+\alpha}(S_c)/\mathbf{R}$ and $H^{-1/2+\alpha}(S_c)$. In other words, there are constants $\gamma_1, \gamma_2 > 0$ such that

$$\gamma_1 \min_{t \in \mathbf{R}} \|f_c - t\|_{H^{1/2+\alpha}(S_c)} \leq \|\rho_c\|_{H^{-1/2+\alpha}(S_c)} \leq \gamma_2 \min_{t \in \mathbf{R}} \|f_c - t\|_{H^{1/2+\alpha}(S_c)} .$$

This is the assertion, because the definition of Sobolev norms implies that

$$\|f_c^\perp\|_{H^{1/2+\alpha}(S_c)} = \min_{t \in \mathbf{R}} \|f_c - t\|_{H^{1/2+\alpha}(S_c)} .$$

□

Theorem 2 *There are constants $\gamma_1, \gamma_2 > 0$ such that*

$$\gamma_1 \|a\bar{\sigma}\|_{H^{-1/2+\alpha}(S)} \leq \|\bar{f}\|_{H^{1/2+\alpha}(S_c)} \tag{18}$$

$$\gamma_2^2 \|a\sigma\|^2_{H^{1/2+\alpha}(S)} \geq a_1^2 \|f_c^\perp\|^2_{H^{1/2+\alpha}(S_c)} + \|\bar{f}_c\|^2_{H^{1/2+\alpha}(S_c)} \tag{19}$$

hold for the solution of (9) with right hand side $f = [f_c, 0]$.

Proof. The estimates are consequences of Theorem 1, Lemma 1 and the convergence of σ to ρ. From (17) it follows that $\bar{\rho}_c = 0$ and combining this with estimate (14) implies $\|\bar{\sigma}_c\|_{H^{-1/2+\alpha}(S_c)} \leq \gamma / a_1 \|\bar{\rho}\|_{H^{-1/2+\alpha}(S)}$. Using (12) we estimate

$$\|a\bar{\sigma}\|^2_{H^{-1/2+\alpha}(S)} = a_1^2 \|\bar{\sigma}_c\|^2_{H^{-1/2+\alpha}(S_c)} + \|\bar{\sigma}_d\|^2_{H^{-1/2+\alpha}(S_d)} \leq \gamma_1 \|\bar{\rho}\|^2_{H^{-1/2+\alpha}(S)} \leq \gamma_2 \|\bar{f}_c\|^2_{H^{1/2+\alpha}(S_c)} ,$$

which implies the first assertion. For the second inequality we estimate

$$\begin{aligned}
\|a\sigma\|^2_{H^{-1/2+\alpha}(S)} &= (a_1^2 - 1)\|\sigma_c\|^2_{H^{-1/2+\alpha}(S_c)} + \|\sigma\|^2_{H^{-1/2+\alpha}(S)} \\
&\geq \gamma_1 a_1^2 \|\rho_c\|^2_{H^{-1/2+\alpha}(S_c)} + \gamma_2 \|f_c\|^2_{H^{1/2+\alpha}(S_c)} \\
&\geq \gamma_1 a_1^2 \|f_c^\perp\|^2_{H^{1/2+\alpha}(S_c)} + \gamma_2 \|\bar{f}_c\|^2_{H^{1/2+\alpha}(S_c)} \\
&\geq \gamma \left(a_1^2 \|f_c^\perp\|^2_{H^{1/2+\alpha}(S_c)} + \|\bar{f}_c\|^2_{H^{1/2+\alpha}(S_c)} \right)
\end{aligned}$$

□

4 Analysis of the Galerkin Method

In this section we describe how the mapping properties of the equivalent charge formulation affect the discretization error of the Galerkin method. The analysis is standard for equations of the type "elliptic plus compact", see, e.g. [3]. However, special care must be taken to demonstrate independence of the parameter λ. To keep the exposition simple we consider only piecewise constant elements on a quasi-uniform mesh. The results can be easily extended to higher order elements.

Denoting by $X_h \subset H^{-1/2}(S)$ the space of piecewise constants on a mesh of width h and by P_h the corresponding L_2-orthogonal projectors, the Galerkin discretization of integral equation (9) can be written in the form

$$(P_h\mathcal{S}_\lambda + P_h\mathcal{K})\sigma_h = P_h f\,. \tag{20}$$

Theorem 3 *For the Galerkin method the error $e_h = \sigma - \sigma_h$ can be bounded by*

$$\|e_h\|_{H^{-1/2}(S)} \le \gamma h \|\sigma\|_{H^{1/2}(S)}.$$

Proof. Since $\mathcal{S}_\lambda$ is elliptic, the operator $S_h = P_h\mathcal{S}_\lambda$ is invertible in X_h. Setting $K_h = P_h\mathcal{K}$, equation (20) can be rewritten in the equivalent form

$$(I + S_h^{-1}K_h)\sigma_h = S_h^{-1}P_h f\,.$$

Subtracting this from (13) gives for the error

$$(I + S_h^{-1}K_h)e_h = \sigma - \tilde{\sigma}_h\,, \tag{21}$$

where $\tilde{\sigma}_h = S_h^{-1}P_h\mathcal{S}_\lambda\sigma$ is the Galerkin solution of $S_h\tilde{\sigma}_h = P_h\mathcal{S}_\lambda\sigma$. Thus the right hand side can be estimated by using standard arguments for elliptic equations

$$\|\sigma - \tilde{\sigma}_h\|_{H^{-1/2}(S)} \le \gamma_1 \inf_{\chi_h \in X_h} \|\sigma - \chi_h\|_{H^{-1/2}(S)} \le \gamma_2 h \|\sigma\|_{H^{1/2}(S)}\,.$$

It remains to verify the stability of $I + S_h^{-1}K_h$. For this, consider the elliptic equation $\mathcal{S}_\lambda\phi = g$ and its Galerkin approximation $S_h\phi_h = P_h g$ for an arbitrary $g \in H^{1/2}(S_c) \times H^{-1/2}(S_d)$. Subtracting the last two equations gives the following expression for the error

$$\phi - \phi_h = (S_h^{-1}P_h - \mathcal{S}_\lambda^{-1})g\,,$$

on the other hand, the standard convergence analysis for elliptic equations yields

$$\|\phi - \phi_h\|_{H^{-1/2}(S)} = \|(S_h^{-1}P_h - \mathcal{S}_\lambda^{-1})g\|_{H^{-1/2}(S)} \le \gamma_1 \inf_{\chi_h \in X_h} \|\phi - \chi_h\|_{H^{-1/2}(S)} \to 0$$

for $g \in H^{-1/2}(S)$. Thus $S_h^{-1}P_h \to \mathcal{S}_\lambda^{-1}$ pointwise and because of the compactness of $\mathcal{K}$ we have $S_h^{-1}P_h\mathcal{K} \to \mathcal{S}_\lambda^{-1}\mathcal{K}$ uniformly as $h \to 0$. Then stability follows from the fact that the operator $I + \mathcal{S}_\lambda^{-1}\mathcal{K}$ is invertible and its norm can be bounded independently of λ. □

Estimate (12) also implies that the condition number of the discretized linear system depends only on the discretization and not on the coefficients. Thus large coefficients cause

no problems for the numerical approximation of the density. However, numerical difficulties may arise for $a\sigma$ when the density is calculated via the equivalent charge formulation (20) and then subsequently multiplied with the coefficient a.

To illustrate this consider solving (5) with a constant right hand side. In this case we see from Theorem 2 that $\|\sigma_c\| = \mathcal{O}(1/a_1)$ and $\|\sigma_d\| = \mathcal{O}(1)$. When integral equation (5) is solved numerically and the solution is subsequently multiplied by the factor a, then the discretization error on S_c grows like a_1 while the solution $a\sigma$ converges to a finite value.

On the other hand, no scaling errors arise for a right hand side orthogonal to the constant functions. From Theorem 2 the solution $a\sigma$ grows like a_1 and hence the relative error will be independent of a. More precisely, from estimates (12) and (19) we have

$$\|a\sigma^\perp\|_{H^{1/2}(S)} \geq \gamma_1 a_1 \|f^\perp\|_{H^{1/2}(S)} \geq \gamma_2 a_1 \|\sigma^\perp\|_{H^{1/2}(S)}$$

and hence

$$\|ae_h^\perp\|_{H^{-1/2}(S)} \leq a_1 \|e_h^\perp\|_{H^{-1/2}(S)} \leq \gamma_1 h a_1 \|\sigma^\perp\|_{H^{1/2}(S)} \leq \gamma_2 h \|a\sigma^\perp\|_{H^{1/2}(S)}\,. \tag{22}$$

5 The Perturbation Approach

The analysis of the Galerkin method shows that large discretization errors of $a\sigma$ come from different scales in the equivalent charge formulation for constant right hand sides. For a right hand side orthogonal to a constant, the density σ_c does not vanish in the limit as $a_1 \to \infty$ allowing discretization errors independent of a_1 as in (22).

In the following we will solve integral equation (5) for $\bar{f}$ and $f^\perp$ separately. The density $\sigma^\perp$ for $f^\perp$ can be determined directly with Galerkin discretization of (5). For the density $\bar{\sigma}$ for $\bar{f}$ we will introduce a perturbation technique which avoids having to solve problems with different scales. The analysis of the method will demonstrate that the discretization error of $a\sigma$ can be bounded independently of the parameter λ.

To obtain this formulation we set up the density $\bar{\sigma}$ for $\lambda < 1$ as a combination of the solution $\bar{\rho}$ for $\lambda = 1$ and a perturbation $\tilde{\sigma}$, i.e.,

$$\bar{\sigma} = \bar{\rho} + \tilde{\sigma}\,.$$

The density $\bar{\rho}$ vanishes on S_c and one could consider solving integral equation (10) only on the interface. However, this results in an integral equation with a non-trivial null space. To avoid this difficulty reconsider boundary value problem (11). Obviously, the potential v is constant throughout D_1 and hence solves the boundary value problem

$$\begin{aligned} \Delta v &= 0 && \text{in } \mathbf{R}^3 \setminus S \\ v &= \bar{f}_c && \text{on } S_d \\ v &= \mathcal{O}(\tfrac{1}{|x|}) && \text{as } |\vec{x}| \to \infty\,. \end{aligned}$$

Thus the density on the interface can be determined from the integral equation

$$V_d \bar{\rho}_d(x) = \bar{f}_c\,, \quad x \in S_d\,. \tag{23}$$

To obtain an integral equation for the perturbation $\tilde{\sigma}$ note that its potential $\tilde{u} = V_c\tilde{\sigma}_c + V_d\tilde{\sigma}_d$ vanishes on S_c. The condition for $\tilde{\sigma}$ on the interfaces can be derived from the jump relation (4) (recall that we have set $a_0 = 1$)

$$a_1 \frac{\partial \tilde{u}^-}{\partial n} - \frac{\partial \tilde{u}^+}{\partial n} = \frac{\partial v^+}{\partial n} - a_1 \frac{\partial v^-}{\partial n} .$$

The right hand side of the above equation simplifies to $\bar{\rho}_d$. Thus the perturbation density solves the following integral equation

$$\begin{array}{rcll} V_c\tilde{\sigma}_c(x) + V_d\tilde{\sigma}_d(x) & = & 0\,, & x \in S_c\,, \\ K_c'\tilde{\sigma}_c(x) + \left(\frac{1}{2\lambda} + K_d'\right)\tilde{\sigma}_d(x) & = & \frac{\lambda-1}{2\lambda}\bar{\rho}_d(x)\,, & x \in S_d\,. \end{array} \tag{24}$$

The discussion above leads to the following description of the perturbation approach

1. Decompose the right hand side $f_c = \bar{f}_c + f_c^\perp$.
2. Solve (20) with right hand side $f_c^\perp$ by Galerkin discretization

$$P_h\left(\mathcal{S}_\lambda + \mathcal{K}\right)\sigma_h^\perp = P_h f_c^\perp\,. \tag{25}$$

3. Solve integral equation (23)

$$P_h V_d \bar{\rho}_{d,h} = \bar{f}_c\,, \tag{26}$$

   and set $\bar{\rho}_h = [0, \bar{\rho}_{d,h}]$.

4. Solve the perturbation equation (24)

$$P_h\left(\mathcal{S}_\lambda + \mathcal{K}\right)\tilde{\sigma}_h = \frac{\lambda-1}{2\lambda}\bar{\rho}_h\,. \tag{27}$$

5. The approximate solution of (5) is given by

$$\sigma_h = \tilde{\sigma}_h + \bar{\rho}_h + \sigma_h^\perp\,.$$

Theorem 4 *For the perturbation method with piecewise constant elements and Galerkin discretization the following error estimates hold for $\lambda_0 < \lambda \leq 1$*

$$\|a(\bar{\sigma} - \bar{\sigma}_h)\|_{H^{-1/2}(S)} \leq \gamma_1 h \|\bar{\sigma}\|_{H^{1/2}(S)}\,, \tag{28}$$

$$\|a(\sigma - \sigma_h)\|_{H^{-1/2}(S)} \leq \gamma_2 h \|a\sigma\|_{H^{1/2}(S)}\,. \tag{29}$$

Proof. The discretization error of $\bar{\rho}$ can be bounded using the standard error analysis of elliptic equations

$$\|\bar{\rho} - \bar{\rho}_h\|_{H^{-1/2}(S_d)} \leq \gamma h \|\bar{\rho}_d\|_{H^{1/2}(S_d)}\,. \tag{30}$$

To account for the approximate right hand side in the perturbation equation (27) we also consider the Galerkin solution $\hat{\sigma}_h$ for the exact right hand side

$$P_h\left(\mathcal{S}_\lambda + \mathcal{K}\right)\hat{\sigma}_h = \frac{\lambda-1}{2\lambda}P_h\bar{\rho} \tag{31}$$

and estimate, using the triangle inequality

$$\|\tilde{\sigma} - \tilde{\sigma}_h\|_{H^{-1/2}(S)} \leq \|\tilde{\sigma} - \hat{\sigma}_h\|_{H^{-1/2}(S)} + \|\tilde{\sigma}_h - \hat{\sigma}_h\|_{H^{-1/2}(S)} \,. \tag{32}$$

A bound for the first term in (32) follows from Theorem 3

$$\|\tilde{\sigma} - \hat{\sigma}_h\|_{H^{-1/2}(S)} \leq \gamma h \|\tilde{\sigma}\|_{H^{1/2}(S)} \,. \tag{33}$$

The second term in (32) satisfies

$$(S_h + K_h)\,(\tilde{\sigma}_h - \hat{\sigma}_h) = \frac{\lambda - 1}{2\lambda}(\bar{\rho}_h - P_h\bar{\rho})\,.$$

Since the right hand side vanishes on S_c, the above equation assumes the equivalent form

$$\left(I + S_h^{-1}K_h\right)(\tilde{\sigma}_h - \hat{\sigma}_h) = (\lambda - 1)(\bar{\rho}_h - P_h\bar{\rho})\,.$$

The stability of $I + S_h^{-1}K_h$ was shown in the proof of Theorem 3, hence we may estimate

$$\|\tilde{\sigma}_h - \hat{\sigma}_h\|_{H^{-1/2}(S)} \leq \gamma_1(1-\lambda)\|\bar{\rho}_h - P_h\bar{\rho}\|_{H^{-1/2}(S_d)} \leq \frac{\gamma_2 h}{a_1}\|\bar{\rho}\|_{H^{1/2}(S_d)} \,. \tag{34}$$

Furthermore, from (12) and (24) it follows that

$$\|\tilde{\sigma}\|_{H^{1/2}(S)} \leq \gamma_2 \frac{1-\lambda}{2\lambda}\|\bar{\rho}\|_{H^{1/2}(S)} \leq \frac{\gamma_3}{a_1}\|\bar{\rho}\|_{H^{1/2}(S)} \,. \tag{35}$$

Combining estimates (14), (30), (33), (34) and (35) the first assertion of the theorem follows from

$$\begin{aligned}
\|a(\bar{\sigma} - \bar{\sigma}_h)\|_{H^{-1/2}(S)} &\leq \|\bar{\rho} - \bar{\rho}_h\|_{H^{-1/2}(S)} + \|a(\tilde{\sigma} - \tilde{\sigma}_h)\|_{H^{-1/2}(S)} \\
&\leq \gamma_1 h\|\bar{\rho}\|_{H^{1/2}(S_d)} + a_1\|\tilde{\sigma} - \tilde{\sigma}_h\|_{H^{-1/2}(S)} \\
&\leq \gamma_2 h\|\bar{\rho}\|_{H^{1/2}(S)} \\
&\leq \gamma_3 h\|\bar{\sigma}\|_{H^{1/2}(S)} \,.
\end{aligned}$$

The second assertion follows from the previous estimate and Theorems 2 and 3

$$\begin{aligned}
\|a(\sigma - \sigma_h)\|^2_{H^{-1/2}(S)} &\leq 2\left(\|a(\bar{\sigma} - \bar{\sigma}_h)\|^2_{H^{-1/2}(S)} + \|a(\sigma^\perp - \sigma_h^\perp)\|^2_{H^{-1/2}(S)}\right) \\
&\leq 2\left(\gamma_1 h^2\|\bar{\sigma}\|^2_{H^{1/2}(S)} + a_1^2\|\sigma^\perp - \sigma_h^\perp\|^2_{H^{-1/2}(S)}\right) \\
&\leq \gamma_2 h^2\left(\|\bar{\sigma}\|^2_{H^{1/2}(S)} + a_1^2\|\sigma^\perp\|^2_{H^{1/2}(S)}\right) \\
&\leq \gamma_3 h^2\|a\sigma\|^2_{H^{1/2}(S)} \,.
\end{aligned}$$

□

6 Numerical Examples

In this section we report some preliminary numerical results obtained by the equivalent charge formulation and the perturbation method. All integral equations are discretized with piecewise constant elements. To simplify the quadrature of matrix entries of the arising linear systems, the surfaces have been replaced by linear triangulations. The additional error introduced by the surface approximation has not been discussed in this article, but can be analyzed using the techniques developed by Nedelec [5].

Two geometries were used for our examples. In the first one the Dirichlet surface and the interface are the ellipsoids

$$\begin{aligned} S_c &= \left\{ x \in \mathbf{R}^3 \,:\, \frac{x_1^2}{4} + \frac{x_2^2}{1} + \frac{x_3^2}{9} = 1 \right\}, \\ S_d &= \left\{ x \in \mathbf{R}^3 \,:\, \frac{x_1^2}{5} + \frac{x_2^2}{2} + \frac{x_3^2}{10} = 1 \right\}, \end{aligned}$$

respectively. The right hand side is the constant function $f_c = 1$. For this geometry the density can be expressed in closed form in terms of ellipsoidal coordinates [2].

Table 1 compares the relative discretization errors $\|ae_{c,h}\|/\|a\sigma_c\|$ of the equivalent charge formulation and the perturbation approach for a wide range of coefficients. For all calculations the same discretization into 768 panels on each surface was used. As it is obvious from the table, the error of the equivalent charge formulation grows linearly with a_1 whereas the error of the perturbation method approaches a finite value as $a_1 \to \infty$.

a_1	2	3	5	10	50	10^2	10^3	10^4
PM	0.0156	0.0167	0.0177	0.0185	0.0193	0.0194	0.0194	0.0194
ECF	0.0131	0.0128	0.0176	0.0434	0.2842	0.5883	6.0668	60.854
L_2	3.9420	4.0319	4.1069	4.1650	4.2127	4.2187	4.2241	4.2246

Table 1: Relative L_2-errors of the equivalent charge formulation (ECF) and the perturbation method (PM) and L_2-norms of the density $a_1\sigma_c$. Two ellipsoids example.

The second example consists of the two concentric spheres

$$\begin{aligned} S_c &= \left\{ x \in \mathbf{R}^3 \,:\, |x| = 1 \right\}, \\ S_d &= \left\{ x \in \mathbf{R}^3 \,:\, |x| = 2 \right\}. \end{aligned}$$

We examine the solution behavior for two different right hand sides

$$\begin{aligned} f_c^{(1)} &= 1 + Y_1^0 + Y_2^0 + Y_3^0, \\ f_c^{(2)} &= 1 + \left(Y_1^0 + Y_2^0 + Y_3^0 \right) / a_1, \end{aligned}$$

where Y_n^m denote the spherical harmonics of degree n and order m. The choice of the geometry and the right hand side allow closed-form expressions of the solution. Since $f_c^{(1)}$

is non-constant, the density $a\sigma$ is large for large a_1 thus hiding the errors of the equivalent charge formulation due to the constant part of $f_c^{(1)}$. As a result, the *absolute* discretization errors of both formulations scale like a_1, however, the *relative* discretization errors remain bounded.

a_1	2	3	5	10	50	10^2	10^3	10^4
				$f_c^{(1)}$				
PM	0.0216	0.0221	0.0225	0.0229	0.0233	0.0234	0.0234	0.0234
ECF	0.0217	0.0221	0.0225	0.0229	0.0234	0.0235	0.0235	0.0235
L_2	27.277	40.270	66.133	130.64	646.32	$1.29{\cdot}10^3$	$1.29{\cdot}10^4$	$1.29{\cdot}10^5$
				$f_c^{(2)}$				
PM	0.0209	0.0209	0.0209	0.0210	0.0211	0.0211	0.0211	0.0211
ECF	0.0210	0.0211	0.0217	0.0253	0.0912	0.1841	1.8795	18.846
L_2	14.233	14.321	14.427	14.540	14.661	14.678	14.694	14.696

Table 2: Relative L_2-errors of the equivalent charge formulation (ECF) and the perturbation method (PM) and L_2-norms of the density $a_1\sigma_c$. Concentric spheres example.

To demonstrate that the perturbation approach gives more accurate results even for non-constant right hand sides we scale the non-constant part in $f_c^{(2)}$ by the factor $1/a_1$. In this case the norm of $a\sigma$ remains bounded and the errors in the equivalent charge formulation due to the constant part of $f_c^{(2)}$ dominate. This effect does not show up in the perturbation method. The results for the second example are summarized in Table 2.

The accurate determination of densities due to constant right hand sides is important for many applications. For instance, the small eigenvalues of capacitance matrices are determined by these densities. We will report on results pertaining multiconductor systems in multiple dielectric materials elsewhere [8].

References

[1] Lesslie Greengard and Monique Moura. On the numerical evaluation of electrostatic fields in composite materials. *Acta Numerica*, pages 379–410, 1994.

[2] Oliver D. Kellogg. *Foundations of Potential Theory.* Dover, New York, 1959.

[3] Rainer Kress. *Linear Integral Equations*, volume 82 of *Applied Mathematical Sciences.* Springer, Berlin, Heidelberg, New York, 1989.

[4] T.A. Manteuffel, S.F. McCormick, and G. Starke. First-order system least squares for elliptic problems with discontinuous coefficients: Finite element approximation and multilevel convergence. In Preparation.

[5] J. Nedelec. Curved finite element methods for the solution of singular integral equations on surfaces in R^3. *Comput. Methods Appl. Mech. Engrg.*, 8:61–80, 1976.

[6] S.M. Rao, T.K. Sarkar, and R.F. Harrington. The electrostatic field of conducting bodies in multiple dielectric media. *IEEE Trans. Microwave Theory Tech.*, 32(11):1441–1448, 1984.

[7] G. Strang and G.J. Fix. *An Analysis of the Finite Element Method.* Prentice-Hall, Englewood Cliffs, N.J., 1973.

[8] Johannes Tausch and Jacob White. Capacitance extraction of 3-D conductor systems in dielectric media with high permittivity ratios. 1997.